

Optimization and physicochemical characterization of polymeric nanoparticles containing tinidazole

Ho Hoang Nhan^{1*}, Le Hoang Hao¹, Ho Thi Thu Hue¹, Phan Thi Thao Ngoc¹

(1) Hue University of Medicine and Pharmacy, Hue University

Abstract

Background: Periodontitis is a chronic bacterial infection destroying tooth-supporting tissues. Like metronidazole, tinidazole (TNZ) is also effective in treating periodontitis. The preparation of polymeric nanoparticles containing TNZ helps to improve the solubility and increase the bioavailability of the drug. **Objectives:** This study aimed to formulate and optimize TNZ nanoparticles and evaluate their physicochemical properties. **Materials and methods:** TNZ, Eudragit RSPO polymer as a carrier were used in this study. TNZ-loaded nanoparticles (TNZ NPs) were prepared by the solvent evaporation - emulsion method. The influence of the factors in the formula and the preparation process of TNZ NPs was investigated and optimized using MODDE 13.0 software. The physicochemical properties of NPs were evaluated by scanning electron microscopy (SEM), X-ray diffraction (XRD), Fourier transform infrared spectroscopy (FT-IR), and *in vitro* drug release. **Result:** The optimal TNZ NPs were spherical in shape, mostly amorphous, with particle size of 179.60 ± 2.20 nm, polydispersity index of 0.149 ± 0.024 , and encapsulation efficiency of $47.49 \pm 0.02\%$. TNZ NPs showed prolonged drug release in phosphate buffer pH 6.8 for up to 24 hours. **Conclusions:** The optimal TNZ NPs would be a promising drug delivery system for periodontitis treatment.

Keywords: tinidazole, nanoparticle, periodontitis.

1. BACKGROUND

Periodontitis, a commonly observed dental condition, is prevalent in Vietnam and other countries worldwide. Epidemiological research has revealed its widespread occurrence, affecting approximately 20 - 50% of the global population. This oral disease is prominent in both developed and developing nations [1]. In Vietnam, dental diseases affect over 90% of the population, with over 80% experiencing permanent tooth decay and more than 60% of children and over 80% of adults suffering from gum inflammation, periodontitis, and gingivitis. Additionally, over 30% of adults have periodontal pockets, causing tooth mobility. Periodontitis, a chronic bacterial infection, destroys the supportive tissues of the teeth. It is primarily caused by gram-negative anaerobic bacteria beneath the gums and is considered one of the two major threats to oral health, leading to tooth loss [1].

Tinidazole (TNZ) is a nitroimidazole antibiotic frequently used in clinical settings to treat periodontitis. TNZ eliminates anaerobic bacteria and protozoa by infiltrating their cells, subsequently disrupting DNA strands or inhibiting DNA synthesis [2]. TNZ possesses potent bactericidal properties at low concentrations, offering broad-spectrum coverage against a wide range of anaerobic bacteria. It exerts rapid antimicrobial activity while exhibiting

minimal drug resistance during treatment [3].

Surgery is a common treatment for periodontitis, but it is often supplemented with antibiotics. Systemic antibiotic use for periodontitis is not recommended due to uncertain drug concentrations at the target site and potential side effects. On the other hand, localized drug delivery systems using nanoformulations allow for lower doses but higher concentrations at the intended site, reducing systemic toxicity and the need for frequent administration. This approach improves treatment adherence and patients' quality of life. Thus, nano-based formulations containing TNZ have potential for localized periodontitis treatment.

Hence, this study was aimed at optimizing polymeric nanoparticles containing TNZ using the solvent evaporation method and characterizing their physicochemical properties.

2. MATERIALS AND METHODS

2.1. Materials

TNZ (purity of 100%, European Pharmacopoeia 10) was from China. Eudragit RSPO was purchased from Evonik, Germany. Dichloromethane, Tween 80, and hydrochloride acid (HCl) (analytical grade) were from China. Poloxamer 407 was obtained from BASF, Germany.

2.2. Methods

2.2.1. Preparation and optimization of nanoparticles containing tinidazole

TNZ NPs were prepared using the solvent evaporation method. Briefly, the drug and polymer were dissolved in dichloromethane to create the oil phase. The surfactant was dissolved in water to form the water phase. The oil phase was gradually added to the water phase at a rate of 1 ml/minute, resulting in an oil-in-water emulsion. The resultant emulsion was homogenized using a probe ultrasonic device (100 W, VCX-130, Sonics and Materials, USA) for 10 minutes at a temperature of 0 - 10 °C. Afterward, the emulsion was gently stirred for 4 hours at room temperature to remove the organic solvent. The resulting nanosuspension was then centrifuged at 5000 rpm (Hermle, Z326K, Germany) for 30 minutes, washed three times with distilled water.

For optimization of TNZ NPs, the formulation and process variables for preparing TNZ NPs were investigated for selecting input variables. The output variables included particle size, polydispersity index (PDI), and encapsulation efficiency (EE).

2.2.2. Characterization of tinidazole-loaded nanoparticles

2.2.2.1. Size and size distribution

The average size (measured as intensity distribution) was determined by the dynamic light scattering (DLS) method using the Zetasizer Lab instrument (Malvern, UK). A 2 ml sample of the prepared nanosuspension was diluted with filtered distilled water (filtered through a 0.2 µm membrane) before size and size distribution PDI measurements.

2.2.2.2. Morphology

The concentrated dispersion of polymeric NPs was diluted and dropped onto aluminum foil. The aluminum foil surface was then allowed to dry at room temperature. Subsequently, the sample was observed using a scanning electron microscope (SEM) (Hitachi S-4800, Japan).

2.2.2.3. X-ray diffraction (XRD) analysis

Powder samples (TNZ, excipients), the physical mixture (PM, with similar component ratios as the produced formulations) were finely ground and evenly spread onto sample holders. The X-ray diffraction spectra of the samples were measured using an X-ray diffractometer (D8 ADVANCE, Bruker, Germany) with a copper K α radiation ($\lambda=1.5406$ Å), reflection angle (2θ) ranging from 10° to 70°, a step size of 0.02°, a total measurement time of 498 seconds per step, a current of 40 mA, and a voltage of 40 kV. The measurements were conducted at a room temperature of 25 ± 2°C [4].

2.2.2.4. Fourier-transform infrared spectroscopy (FT-IR) analysis

Powder samples (TNZ, excipients), PM were finely ground and further mixed with potassium bromide (KBr) powder. The resulting mixture was compressed into thin pellets and scanned in the range of 400 - 4000 cm⁻¹ using a Fourier-transform infrared spectrometer (Shimadzu Prestige-21, Shimadzu, Japan) [5].

2.2.2.5. Assay

TNZ content was quantified using the UV-Vis spectrophotometric method. The test sample was diluted with a 0.1 N HCl solution to a concentration range of 4 to 24 µg/ml. The absorbance was measured at the maximum absorption wavelength of 277 nm.

2.2.2.6. Encapsulation efficiency:

EE was evaluated by the percentage ratio between the TNZ amount in NPs and the total amount of TNZ. The quantification of the free drug content was performed using a centrifugal tube (Molecular weight cutoff-MWCO 10 kDa, Sartorius, UK). Two milliliters of the nanosuspension were precisely withdrawn and centrifuged at 5000 rpm for 30 minutes. The supernatant was collected, and then quantified using the UV-Vis spectrophotometric method. The EE is calculated using the equation (1) [6]:

$$EE (\%) = \frac{W_{total\ drug} - W_{unbound\ drug}}{W_{total\ drug}} \times 100\% \quad (1)$$

(Where $W_{total\ drug}$ and $W_{unbound\ drug}$ are the total weight of drug and free drug, respectively (µg/ml)).

2.2.2.7. In vitro drug release

The drug release was evaluated using dialysis bags (MWCO 12–14 kDa, Visking Tubes, UK). Each dialysis bag containing TNZ suspensions (raw material suspension and nanosuspension with a TNZ amount equivalent to 11 mg TNZ) was placed in a dissolution tester (LOGAN UDT-804, USA, using a stirring apparatus) containing PBS buffer solution (300 ml, pH 6.8) at a temperature of 37 ± 0.5 °C with a stirring speed of 50 rpm. At designated time points, 2 ml of the release medium are taken, and 2 ml of fresh medium were replaced. The amount of released TNZ was determined using the UV-Vis spectrophotometric method described in the quantification section [4, 7].

3. RESULTS

3.1. Preparation and optimization of nanoparticles containing tinidazole

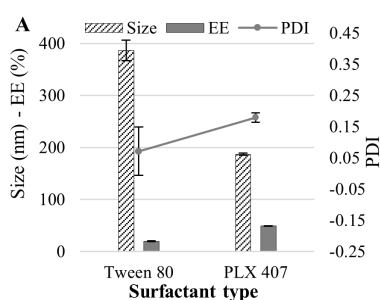
Based on the preliminary studies, several factors in the formulation and manufacturing process were fixed as follows: dichloromethane as organic solvent; a

stirring speed of 1000 rpm; a phase mixing speed of 1 ml/minute; a water/oil ratio of 6:1; an ultrasonication time of 10 minutes; an ultrasonication power of 100 W. Hence, the influence of the remaining critical factors in the formulation and manufacturing process, such as surfactant type, surfactant concentration, polymer concentration, and polymer-to-drug ratio (PL:D), on the physicochemical characteristics of NPs was evaluated.

3.1.1. The influence of surfactant type

TNZ NPs were prepared using two surfactants (Tween 80 and Poloxamer 407 - PLX), while other variables were fixed including Eudragit RSPO concentration of 7 mg/ml, surfactant concentration of 1% (w/v), and PL:D ratio of 3:1 (w/w). The characteristics of the resulting NPs were depicted in Fig. 1A.

It was observed that when using Tween 80, TNZ



NPs had a smaller PDI but a larger particle size (> 250 nm) and a lower EE. On the other hand, when using PLX, TNZ NPs showed a smaller size (< 250 nm), a higher EE, and a PDI below 0.3. Therefore, PLX was chosen as the emulsifier for further studies.

3.1.2. The influence of surfactant concentration

TNZ NPs were prepared using PLX concentrations varied from 0.1% to 0.5% (w/v), while other variables were fixed, including Eudragit RSPO concentrations of 7 mg/ml, and a PL:D ratio of 3:1. The characteristics of the resulting NPs were presented in Fig.1B.

Increasing PLX concentration led to an increase in size, and a decrease in the PDI and EE of TNZ NPs. Hence, the PLX concentration was chosen to be in the range of 0.1% to 0.5% for optimization.

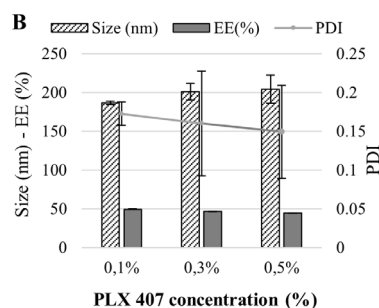
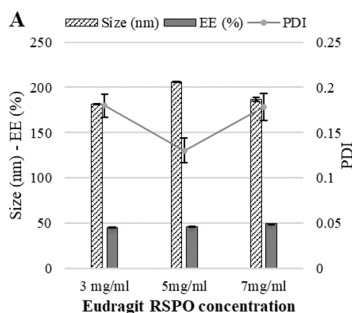


Figure 1. The influence of surfactant type (A) and surfactant (PLX 407) concentration (B) on the physicochemical properties of TNZ NPs

3.1.3. The influence of Eudragit RSPO concentration

TNZ NPs were prepared using Eudragit RSPO concentrations varied from 3 mg/ml to 7 mg/ml while other variables were fixed, including PLX concentration of 1%, and a PL:D ratio of 3:1. The characteristics of the resulting NPs were presented in Fig. 2A.

Increasing Eudragit RSPO concentration led to an increase in particle size and EE, and a decrease in the PDI of TNZ NPs. Hence, Eudragit RSPO concentrations ranging from 3 mg/ml to 7 mg/ml were selected for optimization.



3.1.4. The influence of the polymer:drug ratio

TNZ NPs were prepared using PL:D ratios varied from 3:1 to 7:1, while other variables were fixed, including the PLX concentration of 1%, and Eudragit RSPO of 7 mg/ml. The characteristics of the resulting NPs were shown in Fig. 2B.

Increasing PL:D ratio from 3:1 to 5:1 led to an increase in particle size, PDI, and EE of TNZ NPs. However, further increasing the PL:D ratio from 5:1 to 7:1 led to a decrease in particle size, PDI, and EE of TNZ NPs. Therefore, a PL:D ratio of 3:1 to 7:1 was chosen for optimization.

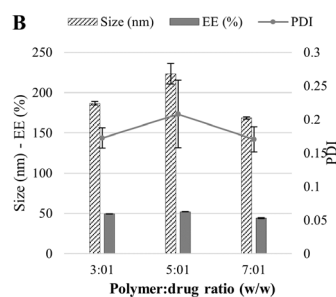


Figure 2. The influence of Eudragit RSPO concentration (A) and polymer:drug ratio (B) on the physicochemical properties of TNZ NPs

3.1.5. Optimization of tinidazole-loaded nanoparticles

For optimization, input variables such as the concentration of PLX surfactant, Eudragit RSPO concentration, and polymer:drug ratio having the impact on the physicochemical properties of TNZ NPs were selected (Table 1). TNZ NPs formulations were designed for D-optimal experimental design using MODDE 13.0 software with their respective responses (Table 2).

Table 1. The levels of independent and dependent variables

	Variable	Symbol	Unit	Low level	High level
The independent variables	PLX 407 concentration	[PLX] (X1)	% (w/v)	1	3
	Eudragit RSPO concentration	[RSPO] (X2)	mg/ml	3	7
	Polymer:Drug ratio (w/w)	PL:D (X3)		3	7
The dependent variables	Size	Size (Y1)	nm	< 250	
	PDI	PDI (Y2)		< 0.3	
	EE	EE (Y3)	%	Max	

Table 2. Formulations of TNZ NPs and their physicochemical characteristics

No.	[PLX]	[RSPO]	PL:D	Size (nm)	PDI	EE (%)
1	0.1	3	3	181.30 ± 0.50	0.180 ± 0.013	45.74 ± 0.38
2	0.5	3	3	202.90 ± 1.20	0.203 ± 0.013	32.83 ± 0.20
3	0.1	7	3	186.80 ± 2.00	0.179 ± 0.015	49.43 ± 0.28
4	0.5	7	3	204.40 ± 18.10	0.149 ± 0.060	44.47 ± 0.18
5	0.3	5	3	192.80 ± 4.10	0.125 ± 0.087	40.73 ± 0.08
6	0.1	3	7	211.80 ± 1.00	0.193 ± 0.019	47.33 ± 0.46
7	0.5	3	7	205.90 ± 18.80	0.139 ± 0.004	34.96 ± 0.69
8	0.5	7	7	208.60 ± 19.30	0.155 ± 0.119	45.16 ± 0.88
9	0.3	7	7	207.10 ± 27.10	0.161 ± 0.067	48.40 ± 1.14
10	0.1	5	7	225.60 ± 13.30	0.218 ± 0.090	47.15 ± 0.36
11	0.3	3	5	225.60 ± 22.40	0.154 ± 0.025	40.95 ± 0.63
12	0.1	7	5	223.70 ± 12.80	0.208 ± 0.050	52.22 ± 0.33
13	0.5	5	5	239.70 ± 14.00	0.130 ± 0.041	38.90 ± 0.21
14	0.3	5	5	231.60 ± 20.30	0.115 ± 0.090	42.99 ± 0.16
15	0.3	5	5	233.30 ± 8.90	0.113 ± 0.043	43.49 ± 0.81
16	0.3	5	5	232.30 ± 14.30	0.120 ± 0.029	42.73 ± 0.19

Based on the data presented in Table 2, TNZ NPs were obtained with size, PDI, and EE ranging from 181.30 to 239.70 nm, 0.113 - 0.218, and 32.83 - 52.22%, respectively. The statistical analysis using MODDE 13.0 software showed that the R² and adjusted R² values for size, PDI, and EE were high (> 0.9). Similarly, the Q² values are also high, indicating the good predictive capability of the model. Furthermore, all the p-values for the regression equations for each response were less than 0.05, and the appropriate p-values (*p* (lack of fit)) were greater than 0.05 for all the response variables.

The polynomial equation represented the

dependence of the output variables on the input variables as follows:

$$Y1 = 13.17 + 0.18X1 + 0.52X3 + 0.27X1X1 - 0.45X2X2 - 1.52X3X3 - 0.39X1X3 \quad (2)$$

$$Y2 = 3.46 - 0.63X1 + 1.02X1X1 + 0.60X2X2 - 0.36X1X2 - 0.58X1X3 + 0.47X2X3 \quad (3)$$

$$Y3 = 8.39 - 0.89X1 + 0.74X2 + 0.16X3 + 0.40X2X2 - 0.29X3X3 + 0.34X1X2 \quad (4)$$

From those data, it was clear that Y1 (size, equation (2)) was influenced by X1 (Poloxamer 407 concentration) (b1 < 0.05), X3 (PL:D ratio) (b3 < 0.05), the quadratic term of X1 (Poloxamer 407 concentration) (b4 < 0.05), the quadratic term of

X2 (Eudragit RSPO concentration) ($b_5 < 0.05$), the quadratic term of X3 (PL:D ratio) ($b_6 < 0.05$), and the interaction between X1 and X3 ($b_8 < 0.05$). On the other hand, Y2 (PDI, equation (3)) was affected by X1 ($b_1 < 0.05$), the quadratic term of X1 ($b_4 < 0.05$), the quadratic term of X2 ($b_5 < 0.05$), the interaction between X1 and X2 ($b_7 < 0.05$), the interaction between X1 and X3 ($b_8 < 0.05$), as well as the interaction between X2 and X3 ($b_9 < 0.05$). For Y3 (EE, equation (4)), it was influenced by X1 ($b_1 < 0.05$), X2 ($b_2 < 0.05$), X3 ($b_3 < 0.05$), the quadratic term of X2 ($b_5 < 0.05$), the quadratic term of X3 ($b_6 < 0.05$), and the interaction between X1 and X2 ($b_7 < 0.05$).

Response surface analysis also shows the impact of the independent variables on the dependent variables (Fig. 3). When the PLX concentration was increased, the size of TNZ NPs increased. When PL:D ratio increased from 3:1 to 5:1, size tended to

increase. However, an increase in PL:D ratio from 5:1 to 7:1 led to a decrease in size. On the other hand, increasing Eudragit RSPO concentration from 3 mg/ml to 5 mg/ml increased the size of TNZ NPs. When the Eudragit RSPO concentration was increased from 5 mg/ml to 7 mg/ml, the size of TNZ NPs decreased (Fig. 3A(1-3)).

Increasing PLX concentration from 0.1% to 0.3% decreased the PDI of TNZ NPs. However, an increase in PLX concentration to 0.5% led to a reversed increase in PDI of TNZ NPs. PDI of TNZ NPs was increased when there was an increase in RSPO concentration and PL:D ratio (Fig. 3B(1-3)).

The EE of TNZ NPs was reduced when PLX concentration was increased. And increasing Eudragit RSPO concentration made EE increase. EE tended to increase when the PL:D ratio was changed from 3:1 to 5:1. EE was decreased again when the PL:D ratio was increased up to 7:1 (Fig. 3C(1-3)).

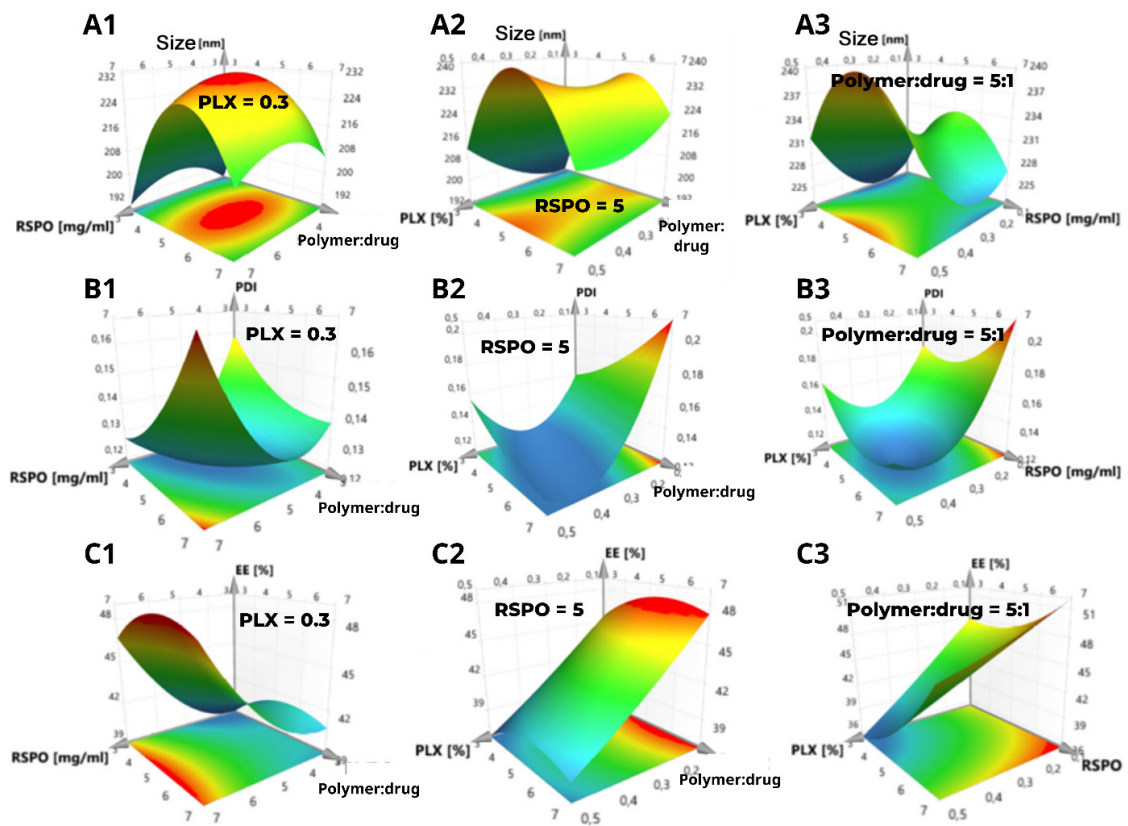


Figure 3. 3D response surface graphs of size, PDI and EE of TNZ NPs

The optimization of TNZ NPs was performed using MODDE 13.0 software. For model validation, TNZ NPs were prepared and characterized following the optimized inputs ($n = 3$) (Table 3).

Table 3. The validity of the optimal formulation of TNZ-loaded nanoparticles

Independent variables			
	[PLX] (%)	[RSPO] (mg/ml)	PL: D (w/w)
Predicted	0.18	7	3
<i>Responses</i>			
	Size (nm)	PDI	EE (%)
Predicted	185.03	0.148	48.46
Observed	179.60 ± 2.20	0.149 ± 0.024	47.49 ± 0.02
Bias	2.93%	0.68%	2.00%

Note: as shown in Table 3, all the deviations were less than 5% for each response, indicating the validity of generated models without the significant difference between the predicted and the actual results.

3.2. Physicochemical characterization of nanoparticles containing tinidazole

3.2.1. Morphology

The morphology of TNZ NPs was determined using SEM (Fig. 4D). The NPs obtained from the optimized formula exhibited a spherical shape, uniform dispersion, and a particle size around 180 nm, which was consistent with the particle size measured by the DLS method (Size: 179.60 ± 2.20 nm, PDI: 0.149 ± 0.024) (Fig. 4C).

3.2.2. X-ray diffraction (XRD)

The X-ray diffraction (XRD) spectrum of TNZ exhibited distinct peaks in the scattering angle range of 10 - 70° at 10.59°, 14.90°, 17.69°, 18.19°, 21.25°, 22.32°, 23.72°, 27.64°, 28.58°, 30.54°, and 32.69°, indicating the crystalline nature of the TNZ raw material [8]. Meanwhile, for the TNZ NPs sample, the diffraction peaks either disappeared or significantly decreased in intensity, although these peaks were still observed in the diffraction pattern of the PM (Fig. 3A). This indicates that TNZ exists in an amorphous state or in a molecularly dispersed form

within the TNZ NPs. The amorphous state of the drug enhances its solubility, thereby contributing to the increased bioavailability of the formulation. The X-ray diffraction evaluation results in this study are consistent with the X-ray diffraction findings in the study conducted by Singh Y et al. [9].

3.2.3. Fourier-transform infrared spectroscopy (FTIR)

TNZ NPs exhibit characteristic peaks in the infrared spectrum corresponding to excipients (Eudragit RSPO shows C=O stretching at 1726.3 cm⁻¹, PLX exhibits -OH stretching at 3441 cm⁻¹), and TNZ raw material displays C-O, C=N, N=O, and S=O stretching vibrations at 1265.3 cm⁻¹, 1523.8 cm⁻¹, 1384.9 cm⁻¹, and 1301.95 cm⁻¹, respectively, indicating no interaction between TNZ and the components in the formulation. In the IR spectrum of TNZ NPs, a peak at 1726.3 cm⁻¹ corresponding to C=O stretching reveals the presence of Eudragit RSPO polymer in the TNZ NPs. The FTIR results for TNZ in this study are consistent with the FTIR results for TNZ reported by Khan et al. [10] (Fig. 4B).

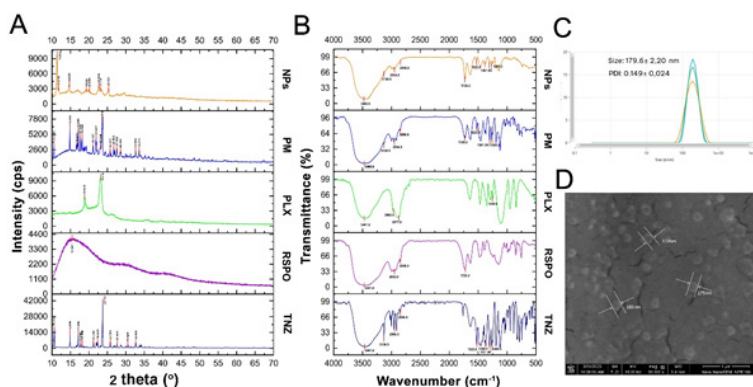


Figure 4. (A) XRD patterns (B) FT-IR spectra of TNZ material, Eudragit RSPO, poloxamer 407, physical mixture (PM), TNZ NPs and (C) Particle size of TNZ NPs by DLS method and (D) Morphology of TNZ NPs by SEM (Scale bar = 1 μm).

3.2.4. In vitro drug release

The drug release (Fig. 5) showed that with raw TNZ powder, the amount of TNZ released in the first 4 hours reached nearly maximum drug content ($96.65 \pm 0.31\%$). In contrast, TNZ NPs exhibited two distinct phases: an initial burst release phase in the first 2 hours, followed by a gradual release phase over the remaining 22 hours, reaching $75.25 \pm 0.75\%$ after 24 hours. This demonstrates that the formulation of TNZ as NPs has altered the drug release capability compared to TNZ raw material.

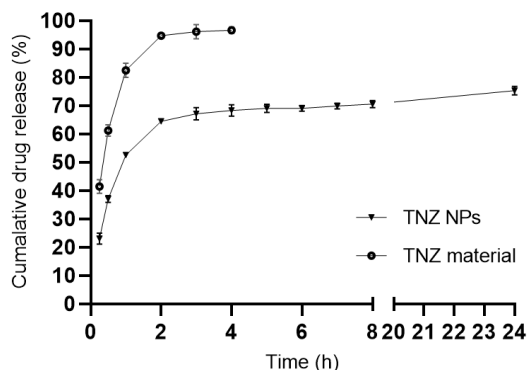


Figure 5. In vitro drug release from TNZ material, TNZ NPs

4. DISCUSSION

Size, PDI, and EE of NPs depend on factors related to the formulation and preparation technique. In this study, the influence of formulation factors on the characteristics of NPs after preparation was evaluated.

Between two types of surfactants, Tween 80 and PLX, it was observed that when Tween 80 was used, the PDI of TNZ NPs was small. However, TNZ NPs using Tween 80 had a large particle size ($>250\text{nm}$) and low EE. On the other hand, when PLX was used as the emulsifier, TNZ NPs had a small particle size ($<250\text{ nm}$), higher EE, and the PDI remained within an acceptable range (<0.3). This could be attributed to the superior stabilizing effect of PLX, which exhibits better adsorption and separation at the interface of emulsion droplets, thereby reducing coalescence through mechanical hindrance and spatial constraints [11]. Furthermore, PLX has a relatively high hydrophilic-lipophilic balance (HLB) value of 18, which is higher than the HLB value of Tween 80 (HLB = 15). This enhances the emulsifying capability of PLX, contributing to the stability of the water phase and reducing the size of the nanoemulsion droplets [12].

Increasing PLX concentration led to an increase in the size of TNZ NPs. This could be explained that a higher concentration of surfactant makes the solution more viscous, making it difficult for the ultrasonic probe to break the droplets into smaller sizes. On the other hand, increasing PLX concentration led to a decrease in the PDI of TNZ NPs. This could be attributed to higher PLX concentration, which helps to reduce surface tension and consequently reduce the aggregation of NPs, resulting in a lower PDI [11]. When increasing the concentration of PLX, it leads to an increase in the solubility of the drug in the aqueous phase. This resulted in a higher amount of free drug, leading to a smaller EE [13].

Increasing Eudragit RSPO concentration led to an increase in size and PDI. This could be due to the increased viscosity of the solution, which hinders the ultrasonic process and leads to aggregation and the formation of larger droplets. As a result, the particle size and the size distribution were increased. However, the resulting nanosystem still maintained a high degree of monodispersity and had a narrow particle size distribution (PDI <0.3) [14-16]. Furthermore, EE was increased as the polymer concentration was increased. This result is consistent with the study by Ansari MJ and colleagues (2019), where increasing the polymer concentration from 1 mg/ml to 10 mg/ml resulted in an increase in EE from 69.10% to 90.80% [17].

Varying PL:D ratio altered the characteristics of TNZ NPs. Decreasing PL:D ratio led to an increase in the drug content and particle size of TNZ NPs with PL:D ratio of 7:1 to 5:1. However, at PL:D ratio of 3:1, the particle size of TNZ NPs was reduced. This result was consistent with the findings of Öztürk Naile and colleagues (2020), where the particle size was increased when the drug content was increased from 0.5 mg to 1 mg, and decreased when the drug content was further increased to 2 mg [18]. EE tended to increase when the PL:D ratio was increased due to the higher amount of PL, which enhanced the drug encapsulation capability and led to improved nanoemulsifying efficiency. PDI showed a gradual increase with the increase in the PL:D ratio. This could be explained by the increased viscosity of the solution, hindering the ultrasonication process and resulting in broader particle size distribution of TNZ NPs.

The predicted results from the D-optimal experimental design for optimization were quite similar to the actual results, with deviations in both size, PDI, and EE below 5%. Additionally, the R^2 , adjusted R^2 , and Q^2 values were all high,

indicating the good predictive ability of the model. The optimized formulation for preparing TNZ NPs consisted of PLX concentration of 0.18%, Eudragit RSPO concentration of 7 mg/ml, and PL:D ratio (w/w) of 3:1.

The morphology of the TNZ NPs under SEM confirmed the consistency with the particle size observed using the DLS method. The X-ray diffraction (XRD) and Fourier-transform infrared spectroscopy (FTIR) spectra indicated that TNZ underwent a transformation from a crystalline state to an amorphous or molecularly dispersed form within polymeric NPs. Furthermore, there was no evidence of chemical interaction between the drug and the excipients in the formulation.

The results of the *in vitro* dissolution study comparing the release profiles between TNZ raw material and TNZ NPs demonstrated that the TNZ raw material achieved nearly maximum drug release (approximately 97%) within the first 4 hours. In contrast, the TNZ polymer nanoparticles exhibited rapid release within the first 2 hours, followed by a gradual release, reaching a cumulative release

of $75.25 \pm 0.75\%$ after 24 hours. These findings indicated an extended drug release capability of the polymer nanoparticle system compared to the TNZ raw material [19].

5. CONCLUSION

TNZ-loaded NPs have been successfully prepared using the solvent evaporation method and optimized using MODDE software. The optimized formulation resulted in spherical TNZ NPs with a mean particle size of 179.60 ± 2.20 nm, PDI of 0.149 ± 0.024 , and EE of $47.49 \pm 0.02\%$. TNZ was transformed from a crystalline state to an amorphous or molecular dispersion within NPs and did not have any interactions with other excipients in the formulation, which was evaluated by FT-IR, XRD spectra. In addition, TNZ NPs exhibited prolonged drug release capability, with a cumulative release of $75.25 \pm 0.75\%$ at 24 hours.

Acknowledgment: This research was funded by Vietnam Ministry of Education and Training of Vietnam (MOET) under Grant no. B2022-ĐHH-19.

REFERENCES

1. Nazir MA. Prevalence of periodontal disease, its association with systemic diseases and prevention. *International journal of health sciences*. 2017;11(2):72.
2. Ministry of Health. Vietnamese National Drug Formulary. Hanoi: Medical Publishing House; 2018.
3. Nord CE. Microbiological properties of tinidazole: spectrum, activity and ecological considerations. *Journal of Antimicrobial Chemotherapy*. 1982;10(suppl_A):35-42.
4. Ho HN, Laidmäe I, Kogermann K, Lust A, Meos A, Nguyen CN, et al. Development of electrospayed artesunate-loaded core-shell nanoparticles. *Drug development and industrial pharmacy*. 2017;43(7):1134-42.
5. Ho HN, Do TT, Nguyen TC, Yong CS, Nguyen CN. Preparation, characterisation and *in vitro/in vivo* anticancer activity of lyophilised artesunate-loaded nanoparticles. *Journal of Drug Delivery Science and Technology*. 2020;58:101801.
6. Nguyen HT, Tran TH, Kim JO, Yong CS, Nguyen CN. Enhancing the *in vitro* anti-cancer efficacy of artesunate by loading into poly-D, L-lactide-co-glycolide (PLGA) nanoparticles. *Archives of pharmacal research*. 2015;38:716-24.
7. Ho HN, Le HH, Le TG, Duong THA, Ngo VQT, Dang CT, et al. Formulation and characterization of hydroxyethyl cellulose-based gel containing metronidazole-loaded solid lipid nanoparticles for buccal mucosal drug delivery. *International Journal of Biological Macromolecules*. 2022;194:1010-8.
8. Madan JR, Dagade RH, Awasthi R, Dua K. Formulation and solid state characterization of carboxylic acid-based co-crystals of tinidazole: An approach to enhance solubility. *Polim Med*. 2018.
9. Singh Y, Vuddanda PR, Jain A, Parihar S, Chaturvedi TP, Singh S. Mucoadhesive gel containing immunotherapeutic nanoparticulate satranidazole for treatment of periodontitis: Development and its clinical implications. *RSC Advances*. 2015;5(59):47659-70.
10. Khan G, Yadav SK, Patel RR, Kumar N, Bansal M, Mishra B. Tinidazole functionalized homogeneous electrospun chitosan/poly (ϵ -caprolactone) hybrid nanofiber membrane: Development, optimization and its clinical implications. *International journal of biological macromolecules*. 2017;103:1311-26.
11. Paulos G, Mrestani Y, Heyroth F, Gebre-Mariam T, Neubert RH. Fabrication of acetylated dioscorea starch nanoparticles: Optimization of formulation and process variables. *Journal of Drug Delivery Science and Technology*. 2016;31:83-92.
12. Kamel AO, Awad GA, Geneidi AS, Mortada ND. Preparation of intravenous stealthy acyclovir nanoparticles with increased mean residence time. *Aaps Pharmscitech*.

2009;10:1427-36.

13. Sharma D, Maheshwari D, Philip G, Rana R, Bhatia S, Singh M, et al. Formulation and optimization of polymeric nanoparticles for intranasal delivery of lorazepam using Box-Behnken design: in vitro and in vivo evaluation. *BioMed research international*. 2014;2014.

14. Nasef AM, Gardouh AR, Ghorab MM. Polymeric nanoparticles: influence of polymer, surfactant and composition of manufacturing vehicle on particle size. *World Journal of Pharmaceutical Sciences*. 2015;2308-22.

15. Cetin M, Atila A, Sahin S, Vural I. Preparation and characterization of metformin hydrochloride loaded-Eudragit® RSPO and Eudragit® RSPO/PLGA nanoparticles. *Pharmaceutical Development and Technology*. 2013;18(3):570-6.

16. Ajiboye AL, Trivedi V, Mitchell JC. Preparation of

polycaprolactone nanoparticles via supercritical carbon dioxide extraction of emulsions. *Drug Delivery and Translational Research*. 2018;8:1790-6.

17. Ansari MJ, Alshahrani SM. Nano-encapsulation and characterization of baricitinib using poly-lactic-glycolic acid co-polymer. *Saudi Pharmaceutical Journal*. 2019;27(4):491-501.

18. Öztürk N, Aslı K, Vural I. Formulation and in vitro evaluation of telmisartan nanoparticles prepared by emulsion-solvent evaporation technique. *Turkish Journal of Pharmaceutical Sciences*. 2020;17(5):492.

19. Sorasitthyanukarn FN, Muangnoi C, Bhuket PRN, Rojsitthisak P, Rojsitthisak P. Chitosan/alginate nanoparticles as a promising approach for oral delivery of curcumin diglutamic acid for cancer treatment. *Materials Science and Engineering: C*. 2018;93:178-90.